Title
The Role of Defects in the Specific Adsorption of Anions on Pt(111)

Author
Ross, P.N.

Publication Date
1990-12-01

LBL-30174
Preprint

Lawrence Berkeley Laboratory
UNIVERSITY OF CALIFORNIA

Materials & Chemical Sciences Division

Submitted to Journal de Chimie Physique

The Role of Defects in the Specific Adsorption of Anions on Pt(111)

P.N. Ross, Jr.

December 1990

Prepared for the U.S. Department of Energy under Contract Number DE-AC03-76SF00098

DISCLAIMER

LBL-30174

THE ROLE OF DEFECTS IN THE SPECIFIC ADSORPTION OF ANIONS ON Pt(111)

LE RÔLE DES DÉFAUTS DANS L'ADSORPTION SPECIFIQUE DES ANIONS SUR Pt(111)

P. N. Ross, Jr.
Materials Sciences Division
Lawrence Berkeley Laboratory
Berkeley, CA 94720

To be published in:

Journal de Chimie Physique - Special Issue on "Electrochemistry at Well Defined Metal Surfaces"

ACKNOWLEDGMENT

The author acknowledges the fine technical assistance of Per Lindberg and Lee Johnson in the conduct of the experiments reported here. Support for this research was provided by the Director, Office of Energy Research, Office of Basic Energy Science, Materials Sciences Division of the U.S. Department of Energy under Contract Number DE-AC03-76SF00098.

LBL-30174

THE ROLE OF DEFECTS IN THE SPECIFIC ADSORPTION OF ANIONS ON Pt(111)

LE RÔLE DES DÉFAUTS DANS L'ADSORPTION SPECIFIQUE DES ANIONS SUR Pt(111)

P. N. Ross, Jr.
Materials Sciences Division
Lawrence Berkeley Laboratory
Berkeley, CA 94720

ABSTRACT

The specific adsorption of anions from hydrochloric and sulfuric acids was studied on Pt(111) surfaces containing two different types of deliberately induced defects. One type of defect surface used was the step-terrace structure produced by cutting a [111] oriented crystal a few degrees off the [111] zone axis. A second type was a randomly up-and-down stepped surface produced by ion bombardment and annealing. The atomic structure of the defect surfaces was determined by spot-profile analysis of LEED patterns in a UHV chamber directly coupled to the electrochemical cell. The vacuum work function of the surfaces was determined by UV photoemission. All of the step defects of the type studied lowered the work function of the surface in direct proportion to the step density, indicative of a local dipole at the step with the positive end of the dipole outward from the surface. The local work function at the step, and thus the local potential of zero charge (pzc), is lower at the step than at the atomically flat terrace. This difference in local pzc controls the coupling of the processes of hydrogen adsorption and anion desorption. On the atomically flat (111) terraces, which have the most positive pzc of all Pt surfaces, the processes are completely decoupled in dilute (mM) acids, with complete desorption of anions from the terraces at potentials more anodic than for the onset of hydrogen adsorption. The lower pzc for steps places the potential region for anion desorption/adsorption in the potential region for hydrogen adsorption/desorption, e.g. anion desorption from steps occurs simultaneously with hydrogen adsorption on the terraces.

RESUME

L'adsorption specifique des anions des acides chlorhydrique et sulfurique à été étudiée sur des surfaces de Pt (111) contenant deux types de défauts induits délibéremment. Un premier type de surface présentant des défauts était constitué par une structure de marches et terrasses produite en écartant le plan de taille d'un cristal orienté (111) de quelques degrés par rapport à l'axe de la zone [111]. Un second type était constitué par des terrasses distribuées au hasard sur différents niveaux, produites par bombardement ionique et recuit. La structure atomique des surfaces contenant ces défauts à été déterminée par l'analyse du profil des taches DEL obtenues dans une chambre à ultra-vide couplée à la cellule électrochimique. Le travail d'extraction sous vide de ces surfaces à été déterminé par photoémission UV. On à trouvé que tous les défauts de type marche étudiés diminuaient le travail d'extraction de façon directement proportionnelle à la densité des marches, indiquant l'existence d'un dipôle local sur la marche, orienté avec son extrémité positive pointant vers l'extérieur. Le travail d'extraction local et par conséquent le potentiel de charge nulle (p.c.n.) local posséde une valeur plus basse sur la marche que sur la terrasse atomiquement plane. Çette difference des p.c.n. détermine le couplage entre les processus d'adsorption del'hydrogene et de désorption des anions. Sur les terrasses (111) atomiquement planes, qui de toutes les surfaces de platine ont le p.c.n. le plus positif, ces processus sont complétement découplés dans les solutions acides diluées (mM) produisant ainsi une désorption complete des anions des terrasses a potentiels plus positifs que celui du début de l'adsorption d'hydrogene. La valeur inférieur du p.c.n. sur les marches situe la région du potentiel de désorption/adsorption des anions dans celle de l'adsorption del'hydrogene, signifiant ainsi que la désorption des anions de ces marches se produit en même temps que l'adsorption del'hydrogene sur les terrasses.

1.0 INTRODUCTION

Cyclic voltammetry on single crystal Pt surfaces, though extensively studied, remains a subject of considerable controversy. The largest member of studies using single crystals were done before the use of UHV surface analytical systems had been developed to the stage where clean transfer of samples from UHV to electrolyte (and

back to UHV) could be achieved [1-4]. Although some of these studies employed surface structure analysis by LEED [2-4] and utilized UHV surface preparation techniques to produce well-ordered surfaces, impurities were picked up during transfer to the electrochemical cell, necessitating electrochemical "cleaning" of the surface by anodic oxidation. It was not appreciated at that time how much roughening was caused by this cleaning procedure, or how sensitive the voltammetry of the (111) surface, in particular, was to surface defects. While the voltammetry of polycrystalline Pt could not be reproduced completely as a simple linear combination of (111), (100) and (110) surfaces, no new features totally outside the envelope of states on polycrystalline Pt were observed, e.g. the major "strongly" and "weakly" bound states of hydrogen on polycrystalline Pt coincided with the largest peaks or Pt(100) and (111), respectively. The assignment of "strongly" bound hydrogen to (100) type sites and "weakly" bound hydrogen to (111) type sites, first made by Will [1], was also consistent with the relative binding energies of hydrogen adsorbed on Pt surfaces in vacuum [5].

This satisfying picture was upset in 1980-2 by a series of papers by Clavilier and co-workers [6-8]. These papers reported new voltammetric features for Pt(111) in the form of highly reversible pseudocapacitive peaks in the double-layer potential region, which had no precedence in polycrystalline work. The Clavilier group used a novel surface preparation technique and a very different

type of Pt single crystal than used in any of the previous studies, which have come to be known as "flame annealed beads". It was reported [6] that just a few cycles of anodic oxidation, as used by others [1-4] to clean the surface, removed the unusual new features. Since the charge under the new features reappeared as charge under the "weak" hydrogen peak, and since the new features were very reversible, Clavilier and co-workers interpreted these features as a new very strongly bound state of hydrogen on atomically flat Pt(111). They attributed the sensitivity of the new features to anodic oxidation to roughening of the surface.

Since only flame annealed beads had produced this voltammetry, there existed the possibility that unique surface structures were produced during the rapid coding and/or quenching, and that these caused the new electrochemistry [9]. However, within a short time several groups using UHV system and LEED analysis with improved sample transfer technology [e.g. 10] were able to reproduce the Clavilier voltammetry with well-ordered (111) surfaces of conventional bulk single crystals [10-13]. Also, using state-of-the-art LEED spot profile analysis [13-14] applied to emersed electrodes, it was shown conclusively that potential cycling through Pt "oxide" irreversibly roughens the (111) surface, and that the new features of Clavilier were indeed unique to atomically flat (111) surfaces. However, several groups disputed the interpretation of the features as "strongly adsorbed hydrogen",

suggesting that in sulfuric and hydrochloric acids they were due to the specific adsorption of anions [12,14-16], and in perchloric acid or hydrofluoric acid they were due to .OH formation [15-16]. Because the origin of these features was unclear, and also due to their uniqueness to the (111) surface, Wagner and Ross [11] referred to these features as "anomalous", a terminology that will be used hereafter in this paper. In a very elegant recent study using in-situ IR spectroscopy, Yeager and co-workers [16] showed convincingly that the anomalous voltammetry on Pt(111) in sulfuric acid is due to the specific adsorption of bisulfate anion.

Independently from the few groups using coupled UHV-electrochemical systems, other groups using the "bead technique" explored the question of the structure sensitivity of the anomalous features using high Miller-index single crystals [18-23] that in principal form step-terrace surface structures [24]. The step-terrace structures enable one to control the terrace length, and thus the distance between defects in the form of monatomic steps. However, there are problems in achieving step-terrace structures with Pt, particularly for (100) and (110) vicinal surfaces. None of the previous studies [18-23] with high Miller-index surfaces used LEED analysis to confirm the formation of the desired step-terrace structures, and most did not even seem to be aware of the extensive study of the stability of high Miller-index surfaces of Pt by Blakely and Somorjai [25]. An exception was the careful

study by Clavilier, Achi and Rodes [23] using crystals cut a few degrees off the [111] zone axis in the direction of the [110] pole, forming the step-terrace structures Pt(S)[m(111)×(111)] in the notation of Lang Joyner and Somorjai [24]. As reported by Blakely and Somorjai [25], these particular high Miller index surfaces are the only ones that do not facet in the presence of oxygen at high temperature, an important requirement for the use of these surfaces with the "bead technique". The study by Clavilier et. al. [23] using [m(111)×(111)] surfaces clearly established that a critical terrace length of at least 9 atoms was required to observe all the details of the anomalous features on Pt(111).

In the present work, we present a study of the role of surface defects in the specific adsorption of chloride and (bi)sulfate anion on Pt(111). Surface defects were deliberately introduced to the (111) surface by two methods. One was simply to ion-bombard the surface in UHV, then only partially anneal the ion damage. The structure of the partially annealed surface was then analyzed quantitatively using LEED spot-profile analysis (SPA) [17]. A second method was to use a series of step-terrace structures, of the type [m(111)×(111)] used previously by Clavilier et. al. [23] with the bead technique. In this case, however, the formation of a true step-terrace structure having the desired terrace length (m) and monatomic step height was determined after UHV surface preparation by LEED. The two types of defect surfaces can be unified

and analyzed quantitatively by the step density, which is the number of monotonic steps appearing per unit length of the surface. The vacuum work function was measured for all the surfaces studied, and it is shown that the step defects lower the work function of the surface in proportion to the step density, indicative of a dipole moment at the step with the positive end of the dipole outward. It is shown that an electrostatic model for specific adsorption of anions at the step accounts for the structure sensitivity of the anomalous voltammetry for the Pt(111) surface in these electrolytes.

2.0 EXPERIMENTAL

The apparatus for the experiments reported here was a directly coupled UHV-electrochemical cell system described in detail elsewhere [10]. The UHV chamber was equipped with a double pass CMA (PHI Model 15-255) which was used for both Auger electron spectroscopy (AES) and UV photoemission spectroscopy (UPS). UV photons were generated using a commercial discharge lamp (PHI Model 1500) operated with either helium or neon. The UV light was not monochromatized. The absolute work function of a particular surface was determined from the width of the photoemission band using He(I) light ($h\upsilon$ = 21.22 eV). The reproducibility of the work function measurements was ± 0.05 eV. The chamber was also equipped with conventional LEED optics.

The details of solution preparation and of the operation of the electrochemical cell were given previously [10-11]. The standard electrolyte used was 0.3 M HF (pH = 2) prepared from Baker Ultrex Grade reagent. Sulfate and chloride anions were added via additions of sulfuric and hydrochloric acid solutions also prepared from Baker Ultrex Grade reagent. All potentials are given versus a normal hydrogen electrode (nhe) in the same electrolyte.

3.0 RESULTS

3.1 LEED analyses of defect surfaces

Two types of defect surfaces were used. The first used were prepared from a Pt(111) crystal that had been pre-cleaned by many cycles of ion bombardment, oxygen dosing, and thermal annealing. The crystal, in the annealed state, produced the sharpest LEED patterns, with a defect density estimated from SPA to be less than 3×10^{6} cm^{-1}. This was the reference surface which we will refer to hereafter as the "atomically flat" or "well-ordered" surface. Rougher surfaces were prepared from this state by ion bombardment and oxygen dosing, but not thermally annealed (the crystal was flashed to desorb oxygen, ca. 600 K, but then rapidly cooled to ambient temperature). The LEED pattern for one surface after that treatment is shown in Figure 1a. This pattern has three sharp spots and three "fuzzy" spots. The fully annealed, well-ordered surface has all six spots sharp, with an FHWM even slightly smaller than that for the sharp spots in Figure 1a. The beam energy in Figure

1a was 76 eV, which is an anti-Bragg condition for coherent scattering of electrons from the successive (111) planes, i.e. scattering from individual (111) planes are out-of-phase with each other and electrons are scattered from each plane into the detector independently from the other planes. The fact that one set of spots is sharp indicates there is one (111) plane of atoms, e.g. the second layer, that has very few defects. The set of broad spots rotated 60° from the sharp spots indicates that the first layer of atoms, which is rotated from the second layer by 60° , has many missing atoms in the layer, creating a stepped surface.

Figure 1b shows the variation in the FWHM of LEED spots with energy. 60 eV and 95 eV are the Bragg energies for in-phase scattering (diffraction) of electrons from successive (111) planes, indicating that the steps in all the surfaces in Figure 1b were predominantly of monatomic height. From the FWHM at the anti-Bragg condition of 76 eV, we can calculate the step density for each surface in Figure 1b using the model of Lu and Lagally [27], as we described previously [14]. The surface for the curve labelled 4 was a randomly up-and-down stepped surface, with mostly monatomic step heights and <u>average</u> step density of ca. 15×10^6 cm^{-1}. This is a very rough surface, produced by electrochemical cycling through oxide formation, and is difficult to describe in terms of a physical model. The surfaces labelled 2 and 3 were heavily ion bombarded then only partially annealed in UHV. They are correlated hole

structures created by the nucleation of isolated vacancies into "holes", (or "pits") i.e. visualize a flat surface from which individual atoms are removed at random (creating isolated vacancies) and then the vacancies coalesce locally to form a hole one atom deep in the original surface. There was a correlation between the size of the hole and the density of holes in these surfaces, with the distance between holes being equal to the average hole diameter. The average hole diameter in these two surfaces was estimated to be ca. 5 and 7 atoms wide, respectively, meaning the average step densities were ca. 9 and 6×10^{6} cm^{-1}. The second type of defect surfaces used were the high Miller-index surfaces (997), (332), (655), (221) and (331), produced by cutting a [111] oriented crystal at increasing angles off the [111] zone axis, in this case towards the [110] zone axis. In principle, this should create a series of step-terrace structures denoted as [m(111)×(111)]. The structure of this particular set of Pt stepped surfaces was studied previously with LEED analysis by Blakely and Somorjai [25]. For surfaces of this type, at the anti-Bragg energies the beams are split rather than broadened, as they are for the randomly stepped and correlated hole structures in Figure 1 since the steps are all aligned along one crystallographic axis. The magnitude of the splitting in reciprocal space is inversely proportional to the step density,

making a determination of the step density from the LEED pattern straightforward. The relation between m, in the notation [m(111)×(111)] and the step density, n_s is given by

$$n_s = 2/\sqrt{3}(m-2/3)d \quad (1)$$

The expected value of m or n_s for a particular crystal can be calculated from the angle of the cut. The particular surface structures we found here, after cleaning and annealing in UHV, produced sharp split spots with m = 9, 7, 6, 5 and 3, which agreed with the values of m expected for the angles of cutting. These are exactly the same results reported by Blakely and Somorjai [25] for crystals cut at these angles and annealed in UHV. In addition, we found that these surfaces are not only stable to thermal annealing, but also to electrochemical cycling within a limited potential region, e.g. 0- 1.0 V (see also the discussion below).

3.2 Cyclic voltammetry in H_2SO_4

The voltammetry for a clean, UHV annealed, well-ordered (by LEED analysis) Pt(111) surface in 0.3 M HF has been reported before [11] and shown here again in Figure 2 as a frame of reference. The addition of H_2SO_4 had no observable effect on the voltammetry curve until a threshold concentration was reached, which was approximately 1 mM. As shown clearly in Figure 3, at this threshold, the anomalous [16] features at 0.6 - 0.8 V disappeared, and are replaced by the complex features occurring between 0.2 - 0.7 V, the potential depending on the sulfate concentration as described previously by

Kolb and co-workers [15]. These features in sulfate containing electrolyte have been attributed to (bi) sulfate adsorption/desorption by a number of research groups [15-18]. As pointed out previously [16], the charge under these anion features is very sensitive to the degree of atomic flatness of the Pt(111) surface, and this is shown more quantitatively than before in Figures 4 and 5. Figure 4 shows the voltammetry for a series of Pt(111) surfaces having various degrees of roughness as quantified by LEED-SPA in Figure 1, and Figure 5 shows the voltammetry on a series of [m(111)×(111)] step-terrace surfaces. Both types of rough surfaces show that the shape of the anion feature changes when the step density reaches a critical value of ca. 6×10^6 cm^{-1}. A further increase in the step density brings a significant loss of charge under the anion feature. The charge lost under the anion feature at 0.4 - 0.7 V appears to recur as charge in the "normal" hydrogen adsorption/desorption potential region between 0 -0.2 V. This apparent redistribution of charge due to step defects in the flat (111) surface is in fact quantitative, as discussion later in section 4.

3.3 Cyclic voltammetry in HCl

The addition of chloride to HF showed a similar threshold effect as sulfate, as seen from the curves in Figure 6 for the well-ordered (111) surface. At a concentration of ca. 1 mM Cl^-, there is a complete disappearance of the anomalous feature at 0.6 - 0.8 V, and

a new feature appearing between 0.2 - 0.6 V, with the potential where the feature appears depending on anion concentration. The curve for 1 mM HCl in 0.3 M HF in Figure 6 is very similar to that reported by Hubbard and co-workers [28] for well-ordered Pt(111) in 10 mM HCl + 0.05 mM $CaCl_2$. As was the case for (bi)sulfate, we attribute the feature at 0.2 - 0.6 V in dilute acid containing mM levels of Cl^- to anion adsorption/desorption. The effect of roughness on the shape and charge under the anion feature was similar to that reported above for (bi)sulfate, i.e. the charge in the potential region 0.2 - 0.6 V was lost and reappeared as charge in the 0 - 0.2 V region in direct proportion to the step density. One difference between the chloride addition and the (bi) sulfate addition is evident from comparison of Figures 3 and 6, at concentrations of the Cl^- anion > 0.1 M the voltammetry in the hydrogen region (0-0.3V) collapses into a single sharp peak at a more cathodic potential than the anion features in (bi) sulfate at the same concentration. As we discuss below, we attribute this difference to the stronger adsorption of Cl^- versus HSO_4^-.

3.4 Work function measurements

As expected, the presence of step-defects in the Pt(111) surface lowered the work-function. The difference in work function, $\Delta\phi$, between the annealed, well-ordered (111) surface and the various rough surfaces was found (Figure 7) to be a linear function of the step density, provided the step density was < 10^7 cm^{-1}. For the

high step densities, the work function lowering by the steps appeared to saturate, with the absolute value of the work function of all surfaces becoming equal to that for the (110) - (2×1) surface (which has a [m (111)×(111)] type structure with m = 2 [5]). The results in Figure 7 essentially extend the previous results of Besocke et. al. [29], who reported $\Delta\phi$ vs. n_s for $n_s < 5 \times 10^6$ cm^{-1}, to step densities of 10^7 cm^{-1}. As pointed out by these authors, the slope of this curve gives via the Helmholz formula [30] the value of the dipole moment at the step, approximately 0.6 Debye for the (111) steps on the [m (111)×(111)] type surfaces, and a slightly larger dipole for steps on the ion-bombarded surfaces. The latter have mixtures of (111)×(111) and (111)×(100) steps, and Besocke et. al. reported dipole moments 20% higher for (111)×(100) steps than for (111)×(111) steps. The sign of the work function change (-) indicates that there is a net (+) positive charge on the step atom.

3.5 LEED analysis of emersed surfaces

LEED analysis of emersed electrodes was conducted in the same manner as before [14] primarily to confirm the stability of the step-terrace surface structures with voltammetric cycling. These stability tests were done mostly in 0.3 M HF, since emersion from this volatile non-adsorbing electrolyte produces a clean surface and sharp LEED pattern for a well ordered sample [14]. For voltammetric cycling within the potential limits of 0- 1.0 V, and for a limit of just ten cycles, the LEED pattern of the emersed

electrode was in all cases identical to the pattern obtained without electrolyte immersion. When LEED analyses were conducted on electrodes emersed from sulfate and chloride containing electrolyte, some striking and important results were observed. Emersion from 0.3 MHF + 5 mM H_2SO_4 at any potential produced an increase in the LEED background intensity and small sulfur and oxygen AES signals, but otherwise the LEED pattern was the same as that for emersion of the same sample from 0.3 MHF without H_2SO_4 added. We did not attempt to quantify the amount of or to determine the nature of the sulfuric acid residue remaining on the surface after emersion. For our purposes, it was sufficient to observe the LEED spots from the Pt surface structure, upon which the presence of sulfuric acid in the electrolyte appeared to have no effect. Emersion of surfaces from HCl containing electrolyte, did, however, produce new patterns. Figure 8a shows the LEED pattern for a well-ordered (111) surface emersed from 0.3 M HF + 1 mM HCl at 0.18 V. There was an increased background with a weak, rather poorly defined p(2×2) superlattice, and a significant Cl AES peak. When the emersion potential was increased to above 0.4 V, just anodic to the voltammetry feature in Figure 6 we attributed to anion adsorption/desorption, the Cl/Pt AES peak ratio doubled, and the LEED pattern changed to the one shown in Figure 8b, with a sharp well-contrasted $(\sqrt{3}\times\sqrt{3})$ R 30° superlattice. Using the Auger calibration factors developed by Wagner and Moylan [31], the Cl/Pt AES ratio was consistent with

the 1/3 coverage indicated by the $(\sqrt{3}\times\sqrt{3})$ R 30° LEED pattern. Thermal desorption spectroscopy (TDS) indicated that the p(2×2) structure from emersion at 0.18 V represents species desorbing as HCl (M/e = 36), whereas the $(\sqrt{3}\times\sqrt{3})$ R 30° structure from emersion at > 0.4 V was just from adsorbed Cl, desorbing as Cl (M/e = 35) at ca. 950° K.

Emersion of the same crystal from higher concentrations of HCl resulted in a loss of the $(\sqrt{3}\times\sqrt{3})$ R 30° pattern but with roughly constant Cl/Pt AES ratio. Emersion from 0.1 M HCl resulted in only a diffuse LEED pattern, and TDS indicated the major species desorbing was HCl, however some amount of Cl was observed (desorbing at 950° K) as well. A quantitation of the relative amounts of HCl/Cl was not attempted. These observations from 0.1 M HCl were independent of potential.

4.0 DISCUSSION

A number of the results reported here are not new, and some are in fact merely reproductions or extensions of prior work by others. Specifically, the work function measurements reported here for the [m(111)×(111)] step-terrace structures primarily confirm and extend the prior measurements by Besocke et. al. [29] to smaller m (higher n_s). However, the saturation of $\Delta\Phi$ above a critical step density is a new observation and has important implications, as we discuss below. The voltammetry curves for the [m(111)×(111)] structures in sulfuric acid were reported previously by Clavilier et. al. [23],

and the curves we report here are essentially identical to the curves reported by them. However, there was value to repeating these experiments, since Clavilier et. al. did not have a UHV/LEED system to prepare and characterize their surfaces, as we have done here.

We have assigned the voltammetry features occurring on well-ordered Pt(111) in dilute (mM) sulfuric and chloride acids in the potential region between hydrogen adsorption and oxide formation as due to anion adsorption/desorption. In sulfuric acid, direct evidence for this assignment is provided by the in-situ IR spectroscopy of Faguy et. al. [17], but there is lingering controversy over the charge associated with the process [32]. In the case of chloride electrolyte, there is no direct evidence available yet by in-situ spectroscopy which identifies these features as an anion process. However, the ex-situ analysis by LEED/AES reported both here and by Stern et. al. [28] indicates this is a reasonable assignment, particularly from the striking potential dependence of the LEED pattern and the Cl/Pt AES peak ratio. Stern et. al. also assigned the voltammetry feature on Pt(111) at ca. 0.4 V in dilute acid chloride to anion adsorption/desorption on the basis of their ex-situ LEED analysis. One difference between our result here and theirs is the actual LEED pattern. We observed a $(\sqrt{3}\times\sqrt{3})$ R 30° pattern at 1/3 coverage, while they observed a (3×3), to which they assigned a coverage of 2/9. A (3×3) pattern was reported by Erley

[33] for Pt(111) - Cl produced by Cl_2 dosing in UHV. It is not clear why we observed a higher coverage Cl structure than Stern et. al. did in very similar experiments, although the electrolyte compositions were slightly different.

The presence of steps in the atomically flat (111) surfaces reduces the charge under the anion fracture and produces new charge in the hydrogen adsorption region, 0 -0.2V. Clavilier et. al. [23] analyzed this charge balance in detail, and found it to be quantitatively 1:1. This charge balance led these authors to conclude that the voltammetry fractures we have assigned here to anion adsorption/desorption they assigned to hydrogen desorption/adsorption. Their reasoning being that as the concentration of adsorbing anions like chloride and sulfate increase, the anions reduce the binding energy of the adsorbed hydrogen, resulting in the shifting of charge from strongly bound hydrogen (0.3 - 0.7 V) to weakly bound hydrogen (0 -0.2V). We offer here another explanation of this charge shift/balance in terms of anion adsorption [16] and account for the effect of steps on this process in terms of the concept of the local work function.

It is well established that the potential of zero charge (pzc) of a metal electrode surface is directly related to the vacuum work function [34]. One of the expressions frequently used for this relation for a metal M having the crystal plane (hkl) at the metal-solution interface is,

$$E_{\sigma=0}^{(hkl)} = \Phi^{(hkl)}/e - [\delta\chi^{(hkl)} + g_M^S(hkl)]_{\delta=0} + K \qquad (2)$$

where $[\delta\chi^{(hkl)} + g_m^s(hkl)]\sigma = 0$ represents the potential drop at the M(hkl) - solution interface, arising from a change $\delta\chi$ in the electronic structure of the metal due to the contact with water and the dipole contribution $g_M^S(hkl)$ for water molecules at the surface, and K is a constant due to the potential drop at the reference electrode - solution interface. If we want to compare the pzc for different crystal planes of the same metal, then to a first approximation this difference is just

$$E_{\sigma=0}^{(hkl)} - E_{\sigma=0}^{(h'k'l')} = \Phi^{(hkl)} - \Phi^{(h'k'l')} \qquad (3)$$

if we assume that the $\delta\chi$ and g_M^S terms are not very different between different crystal faces (see for example the discussion by Lecoeur et. al. [35] on this point). If we use the well-ordered (111) surface as the reference surface, since it has the highest vacuum work function, then this surface has the most anodic pzc, and all other Pt surfaces as well as (111)-stepped surfaces will all have pzc's at lower potentials. Using entirely UHV measurements, Wagner [36] has estimated the pzc of Pt (111) at pH = 2 as 0.7 ± 0.2 V (versus nhe). Using the $\Delta\Phi$ values we measured this study, we can estimate the pzc for very rough surfaces like those in Figure 3 with $n_s > 10^7$ cm^{-1} as ca. 0.1 V. For dilute anion concentration, we would expect anion adsorption (at low coverage) to occur near the pzc, perhaps slightly cathodic to the pzc if the anion is

strongly chemisorbed. Thus, in contrasting well-ordered (111) voltammetry in dilute (mM) acid to voltammetry for very stepped surfaces, we would expect the anion features to be shifted by approximately the difference in work function, ca. - 0.6 V, and that is consistent with the shifts in charge in Figure 3 and 4 between the regions 0.3-0.7 V and 0-0.2 V.

For the [m (111)×(111)] surfaces, when m > 5, the $\Delta\Phi$ values vary linearly with the step density, implying that the pzc, and thus the potential at which anion features appear, should shift with varying m. That was experimentally not the case. However, the problem occurs in applying macroscopic measurements like the work function and the pzc to a phenomenon like anion adsorption that may be sensitive to localized electron density fluctuation. The work function measurement integrates the charge density distribution over the entire surface, and thus tends to underestimate the true value of surface dipoles [37] caused by heterogeneities in the surface. A more physically significant measure of the pertubation of the electron density distribution at a step is a method which is site specific, i.e. probes the local work function (and thus the local pzc) [38].

There are two methods which probe the local work function at surfaces, scanning tunneling microscopy (STM) and photoemission from adsorbed xenon (PAX). Recently Marchon et. al. [39] found the work function at steps in the Re (0001) surface to be ca. 0.5 eV

lower than at the flat terraces. Alnot et. al. [40] measured the local work function of steps on Pt (111) using PAX. The steps were introduced both by evaporating Pt submonolayer "islands" onto the well-ordered surface, or roughening the surface by ion-bombardment, as we did here. The local work at the step they found to be ca. 0.6 eV lower than the work function of the flat surface. In both instances, the value of the local work function was independent of the step density. If we use these values of local work function, a very consistent interpretation of the effect of steps on the potential for and integral charge under the anion adsorption/desorption features can be fashioned. At a step, the local work function, and thus the local pzc, is ca. 0.5-0.6 V lower than at the atomically flat terrace, and this difference is essentially independent of step density. Thus, anions are desorbed from steps at potentials 0.5-0.6 V cathodic to potentials for desorption from terraces, regardless of the number of steps. As the step density increases, the charge for desorption from steps increases, thereby increasing the charge under the feature that is cathodically shifted from the feature for the flat terrace. The balance of charge between the two features is due primarily to the material balance, i.e. the addition of one step atom "covers" one terrace atom.

The existence of a critical terrace length necessary to observe the anion features due to the terrace can also be explained in terms of the local work function concept. From Figure 6, and also indicated in the report by Clavilier et. al. [23], the critical terrace length is ca. 5-6 atoms, which is also the terrace length where the macroscopic work function (Figure 7) is equal to the local work function at the step. As we shall describe below, the pertubation in the electron density at the surface due to a step-discontinuity causes a significant redistribution of charge at the step atom and a lessor but non-trivial redistribution to the nearest-neighbor and next-nearest-neighbor. These "fields" of disturbance originating at steps will overlap when the steps are separated by ca. 5-6 atoms, and cause the local-work function of the terrace atoms to be lowered and approach the local work function at the step. Hence, the integral (macroscopic) work function becomes equal to the local work function.

The electronic theory of surface dipoles at steps, and the lowering of the work function of a surface due to steps, has its origin in the very early theories of Smoluchowski [41], who postulated a "smoothing effect" of the electron density at atoms of reduced coordination. Our representation of this idea for step-terrace structures is shown qualitatively in Figure 9. By this effect, positive charge accumulates at the step atom leading to a dipole moment that decreases the work function. A modern-day

self-consistant calculation by Lang and Kohn [42] gave Smoluchowski's physical concept a rigorous quantum mechanical basis. Specific quantum theory calculations for the effect of steps on the potential field at a Pt surface were made by Falicov and co-workers [43]. They showed that the presence of a wedge-shaped boundary in a metal with itinerant electrons causes a strong enhancement in Fiedel oscillations near the edge. A Pt ion placed in the neighborhood of the edge feels a local potential that is sizeably different from both a bulk atom and a planar surface atom. The magnitude of this potential difference was 0.35 eV. The local field created by this potential difference splits the d levels of the edge atom and causes charge transfer from d orbitals localized on the edge atom to the delocalized s-band in the bulk. The magnitude of the charge transfer (q in Figure 9) was estimated to be 0.25 e. The calculated lowering of the local work function at the Pt step edge of 0.35 eV is in reasonable agreement with the value of 0.65 eV recently measured by PAX [40]. It should also be noted that the Friedel oscillations [43] are not confined to just the atom at the edge, and the enhancement extends away from the edge out to ca. 5 Å.

So far we have only related the anion adsorption/desorption process to the local work function/pzc in a very qualitative way, by saying that anion adsorption should occur at a given type of surface site when the electrode potential is at (or anodic to) the local pzc, and desorption will occur from that site when the electrode

potential is made sufficiently cathodic of the local pzc, depending on chemical bonding. We can make this relation more rigorous and the discussion more complete, by considering these interactions more quantitatively in terms of the electronic theory just discussed. Consider, as in Figure 10, a jellium metal with a periodic step-terrace structure immersed in an electrolyte containing anions and cations that do not interact strongly with the metal, i.e. ignore all chemical interactions and consider only electrostatic interactions. In vacuum, the metal has a net position charge at the step edge, the excess negative charge being dispersed across the rest of the surface (and to the bulk). When immersed in solution, anions will be adsorbed at the step edges to counter the positive charge there, but only a water layer will form next to the terrace atoms, since the delocalization of the charge transferred from step atoms results in a negligible (screened) charge density at the terrace surface. Therefore the rest (immersion) potential will be equal to the local pzc of the terraces. If the electrode is biased anodically from this potential, anions will be adsorbed on the terrace as well as on the steps. If the electrode is biased cathodically, for a small bias, cations are adsorbed on the terraces

ion adsorption in this model refers to a partially de-solvated ion located close to the jellium edge

while anions remain at steps, due to the potential difference between the terrace and the step. At a larger cathodic bias, the anions are displaced from the steps and replaced by cations.

This purely electrostatic model is sufficient to account for the structure specificity of sulfate and chloride anion adsorption on Pt(111). Referring to the results in Figure 5, for example, the rest potential for the clean well-ordered Pt(111) surface in this electrolyte was ca. 0.4 V. An anodic bias to 0.7 V results in an anodic charge due to adsorption (with charge transfer) of HSO_4^- anions [17] on the flat (111) surface, as shown by the shaded portion of Figure 5c. A cathodic bias to 0 V results in cathodic charge due to cation adsorption (with charge transfer), in this case hydronium ion adsorption to adsorbed hydrogen atoms. In the case of a stepped Pt(111) surface, as in Figures 5a and b, one sees new features (shaded regions) that can be accounted for entirely by the model in Figure 10. If the step density is low, as for [m(111)×(111)] structures with $m \geq 6$, immersion results in spontaneous adsorption of anions at the steps, but the rest (immersion) potential would still be ca. 0.4 V, equal to the local pzc of the terraces ($E_{\sigma=0}^{terrace}$). Anodic bias to 0.7 V produces charge due to anion adsorption on the terraces, but the charge is lower than on the flat (111) surface due to the presence of steps and the reduced number of terrace sites. Cathodic bias from $E_{\sigma=0}^{terrace}$ produces two cathodic charges, in addition to the charge for hydrogen adsorption on the (111) terrace

sites there is charge from anion desorption from the step sites. This accounts for all the features in Figure 5. If the step density is high, as for m $\leq$ 5, there is spontaneous anion adsorption on all parts of the surface, and $E_{rest} \cong E_{\sigma=0}^{terrace} \cong E_{\sigma=0}^{step}$. Thus, anodic bias from the rest potential does not produce any adsorption charge. Cathodic bias from the rest potential produces primarily one charge feature, that from anion desorption from steps co-incident with hydrogen adsorption at the step. This model accounts for all the features in Figure 5.

While the local work function (local pzc) concept and the electrostatic model presented above provides a reasonable explanation of the potential dependence of anion adsorption/desorption processes and the relation to surface defects, it does not explain some of the details of the processes. The 1:1 correspondence between the charge lost on the terraces and gained on the steps as the step density increases [23] is a problem to account for in this model. It is probable that desorption of anions from the step at 0-0.2 V is accompanied by simultaneous adsorption of hydrogen, whereas desorption of anions from the terraces is <u>not</u>. Hence, in simple terms one might expect a 2:1 correspondence, or at least a greater than 1:1 relation, between the two types of sites. However, the amount of charge transfer upon anion adsorption need not be the same at step sites as at terrace sites, and this may compensate for the difference, but it implies smaller charge

transfer at step sites than at terrace sites. The shape of the anion adsorption/desorption features on the well-ordered Pt(111) surface is very similar to those observed on Au(111) [44], but the shape of the features attributed to adsorption/desorption at steps is very different. Again, this difference could be due to the coupling of anion desorption with hydrogen adsorption at steps and not at terraces, but that is unclear at this time.

5. CONCLUSION

One of the most persistent difficulties in understanding the anomalous voltammetry of Pt(111) has been the unique sensitivity of the anomalous features to the atomic flatness of the surface [16]. The local work function (pzc) concept and the electrostatic model developed here provides an explanation for this unique sensitivity. The local work function at a defect in the (111) surface is lower than the work function of the surrounding flat area. Thus, the local potential of zero charge (pzc) at the defect is cathodic to the pzc of the flat area. This difference in pzc controls the coupling of the processes of hydrogen adsorption and anion desorption. On the atomically flat regions, having the most anodic pzc of all Pt surfaces, the processes are completely decoupled in dilute (mM) acids, with complete desorption of anions occurring at potentials more anodic than for the onset of hydrogen adsorption. The cathodic shift of the local pzc at defects places the potential region for anion desorption in the potential region for hydrogen

adsorption, so that anion desorption from defects occurs simultaneously with hydrogen adsorption. The latter process is common to all Pt surfaces other than well-ordered (111), since it is only this surface in which the processes are decoupled due to its very anodic pzc (high work function).

6. ACKNOWLEDGMENT

The author acknowledges the fine technical assistance of Per Lindberg and Lee Johnson in the conduct of the experiments reported here. Support for this research was provided by the Director, Office of Energy Research, Office of Basic Energy Science, Materials Sciences Division of the U.S. Department of Energy under Contract Number DE-AC03-76SF00098.

7. REFERENCES

1. F.G. Will, J. Electrochem. Soc., 112 (1965) 451.

2. A.T. Hubbard, R.M. Ishikawa and J. Katekaru, J. Electroanal. Chem., 86 (1978) 271.

3. K. Yamamoto, D.M. Dolb, R. Kotz and G. Lehmpfuhl, J. Electroanal. Chem. 96 (1979) 233.

4. P. Ross, J. Electrochem. Soc., 126 (1979) 67.

5. P. Ross, Surf. Sci., 102 (1981) 463.

6. J. Clavilier, R. Faure, G. Guinet and R. Durand, J. Electroanal. Chem. 107 (1980) 205.

7. J. Clavilier J. Electroanal. Chem., 107 (1980) 211.

8. J. Clavilier, D. Armand and B.L. Wu, J. Electroanal. Chem., 135 (1982) 159.

9. C.L. Scortichini, F.E. Woodward and C.N. Reilley, J. Electroanal. Chem. 139, (1982) 265.

10. P. Ross, Jr. and F. Wagner in H. Gerischer and C.W. Tobias (Eds.) Advances in Electrochemistry and Electrochemical Engineering, Vol. 13, Wiley, New York, 1985, pp. 69-112.

11. F. Wagner and P. Ross, J. Electroanal. Chem., 150 (1983) 141.

12. M. Markovic, M. Hanson, G. McDougall and E. Yeager, J. Electroanal. Chem., 214 (1986) 555.

13. D. Aberdam, R. Durand, R. Faure and F. El-Omar, Surf. Sci., 171 (1986) 303.

14. F. Wagner and P. Ross, Surf. Sci., 160 (1985) 305.

15. K. Al-Jaaf-Golze, D.M. Kolb and D. Scherson, J. Electroanal. Chem. 200 (1986) 353.

16. F. Wagner and P. Ross, J. Electroanal. Chem. 250 (1988) 301.

17. P. Faguy, N. Markovic, R. Adzic, C. Fieiro and E. Yeager, J. Electroanal. Chem. 289 (1990) 245.

18. B. Love, K. Seto and J. Lipkowski, J. Electroanal. Chem., 199 (1986) 219.

19. J. Clavilier, D. Armand, S.G. Sun and M. Petit, J. Electroanal. Chem., 205 (1986) 267.

20. R. Adzic, A. Tripkovic and V. Vesovic, J. Electroanal. Chem. 204 (1986) 329.

21. S. Motoo and N. Furuya, Ber. Busenges. Phys. Chem., 91 (1987) 457.

22. N.M. Markovic, N.S. Marinkovic and R.R. Adzic, J. Electroanal. Chem., 241 (1988) 309.

23. J. Clavilier, K. Achi and A. Rodes, J. Electroanal. Chem. 272 (1989) 253.

24. B. Lang, R. Joyner and G. Somorjai, Surf. Sci., 30 (1972) 440.

25. D. Blakely and G. Somorjai, Surf. Sci., 65 (1977) 419.

26. M.G. Lagally, in: Chemistry and Physics and Solid Surfaces IV, Springer Series in Chemistry and Physics, Vol. 20, Eds. R. Vanselow and R. Howe (Springer, Berlin, 1982) p. 281.

27. T.-M. Lu and M. Lagally, Surface Sci. 120 (1982) 47.

28. D. Stern, M. Baltruschat, M. Martinez, J. Stickney, D. Song, S. Lewis, D. Frank and A. Hubbard, J. Electroanal. Chem. 217 (1987) 101.

29. K. Besocke, B. Krahl-Urban and M. Wagner, Surf. Sci. 68 (1977) 39.

30. J. Holzl, G. Porsch and P. Schrammen, Surf. Sci. 97 (1980) 529.

31. F. Wagner and T. Moylan, Surf. Sci. 216 (1989) 361.

32. E. Krauskopf, L. Rice and A. Wieckowski, J. Electroanal. Chem. 244 (1988) 347.

33. W. Erley, Surf. Sci. 94 (1980) 281.

34. S. Trasatti, J. Electroanal. Chem. 33 (1971) 351.

35. J. Lecoeur, J. Bellier and C. Koehler, Electrochim. Acta, 35 (1990) 1383.

36. F. Wagner, Physical Chemistry Dept., General Motors Research Laboratories, Warren, MI 48090-9055, private communication.

37. see, for example: J. Holzl and F. Schulte, Work Function of Metals, Vol. 85 of Solid State Physics (Springer-Verlag. Berlin, 1980).

38. K. Wandelt, J. Vac. Sci. Technol. A2 (1984) 802 and references therein.

39. B. Marchon, D. Ogletree, M. Selmeron and W. Siekhaus, J. Vac. Sci. Technol. A6 (1988) 531.

40. M. Alnot, J. Eberhardt and J. Barnard, Surf. Sci. 208 (1989) 285.

41. R. Smoluchowski, Phys. Rev. (1941) 661.

42. N. Lang and W. Kohn, Phys. Rev. B3 (1971) 1215.

43. L. Kesmodel and L. Falicov, Sol. State Comm. 16 (1975) 1201; Y. Tsang and L. Falicov, J. Phys. C (Sol. State Phys.) 9 (1976) 51.

44. D. Scherson and D. Kolb, J. Electroanal. Chem. 176 (1984) 353.

8. FIGURE CAPTIONS

Figure 1. (a) LEED pattern at 76 eV for roughened Pt(111) surface; (b) spot profile analysis (SPA) of (01) LEED beams from: (1) well-ordered, fully annealed surface; (2,3) an ion-bombarded and partially annealed surface; (4) electrochemically roughened surface.

Figure 2. Cyclic voltammetry of a well-ordered Pt(111) surface in 0.3 M HF after immersion under potential control at 0.5 V. 100 mV/s. From [11].

Figure 3. Cyclic voltammetry of a well-ordered Pt(111) crystal in 0.3 M HF with sulfuric acid additions. First complete cycle after immersion at 0.5 V. 50 mV/s.

Figure 4. Cyclic voltammetry in 0.3 M HF + 5 mM H_2SO_4 for (111) surfaces of varying atomic roughness. Labels 1-4 as in Figure 1. All curves shown are first complete cycle after immersion at 0.5 V. 50 mV/s.

Figure 5. Cyclic voltammetry of Pt(s) [m(111)×(111)] step-terrace surface structures in 0.1 M H_2SO_4. First complete cycle after immersion at 0.5V. 50 mV/s. Shaded region in 5c is attributed to anion adsorption; shaded regions in (a) and (b) are changes in curves relative to that in (c).

Figure 6. Cyclic voltammetry of well-ordered Pt(111) in 0.3 M HF with additions of HC1.

Figure 7. The difference in work function, $\Delta\Phi$, between a well annealed Pt(111) surface and a stepped surface as a function of step density. Open circles are for [m(111)× (111)] type structures while dark circles are for randomly stepped structures.

Figure 8. (a) LEED pattern at 85 eV for well-annealed Pt(111) electrode after emersion from 0.3 MHF and 5 mMHC1 at 0.18 V;
(b) LEED pattern for same surface after emersion at 0.78 V.

Figure 9. Model of "smoothing" of the nearly-free electron density across a monatomic step creating a surface dipole. After Smoluchowski [41].

Figure 10. Jellium model representing the electrostatic interactions between the inhomogeneous electron density distribution at a step-terrace surface and ions in solution.

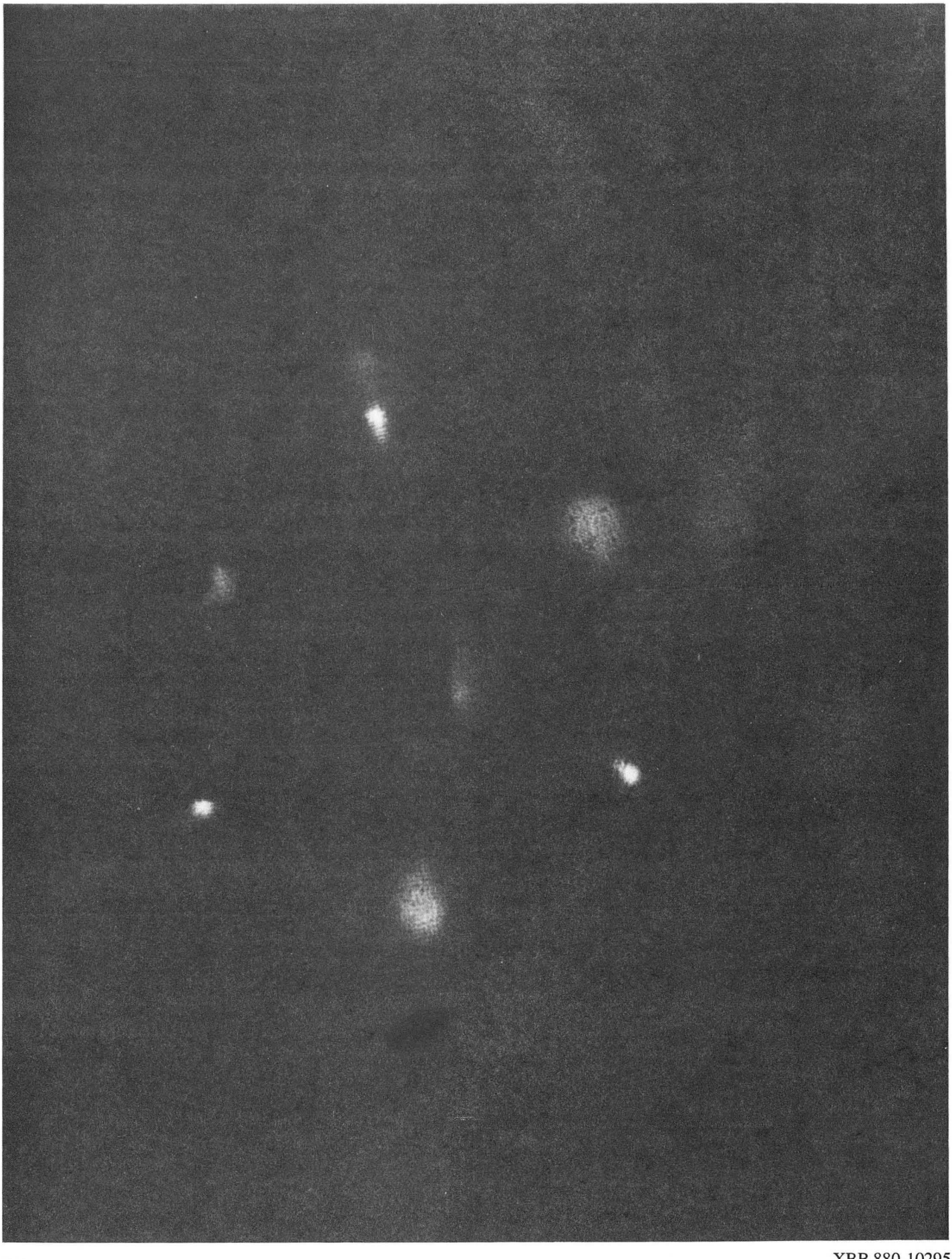

Figure 1a

XBB 880-10295

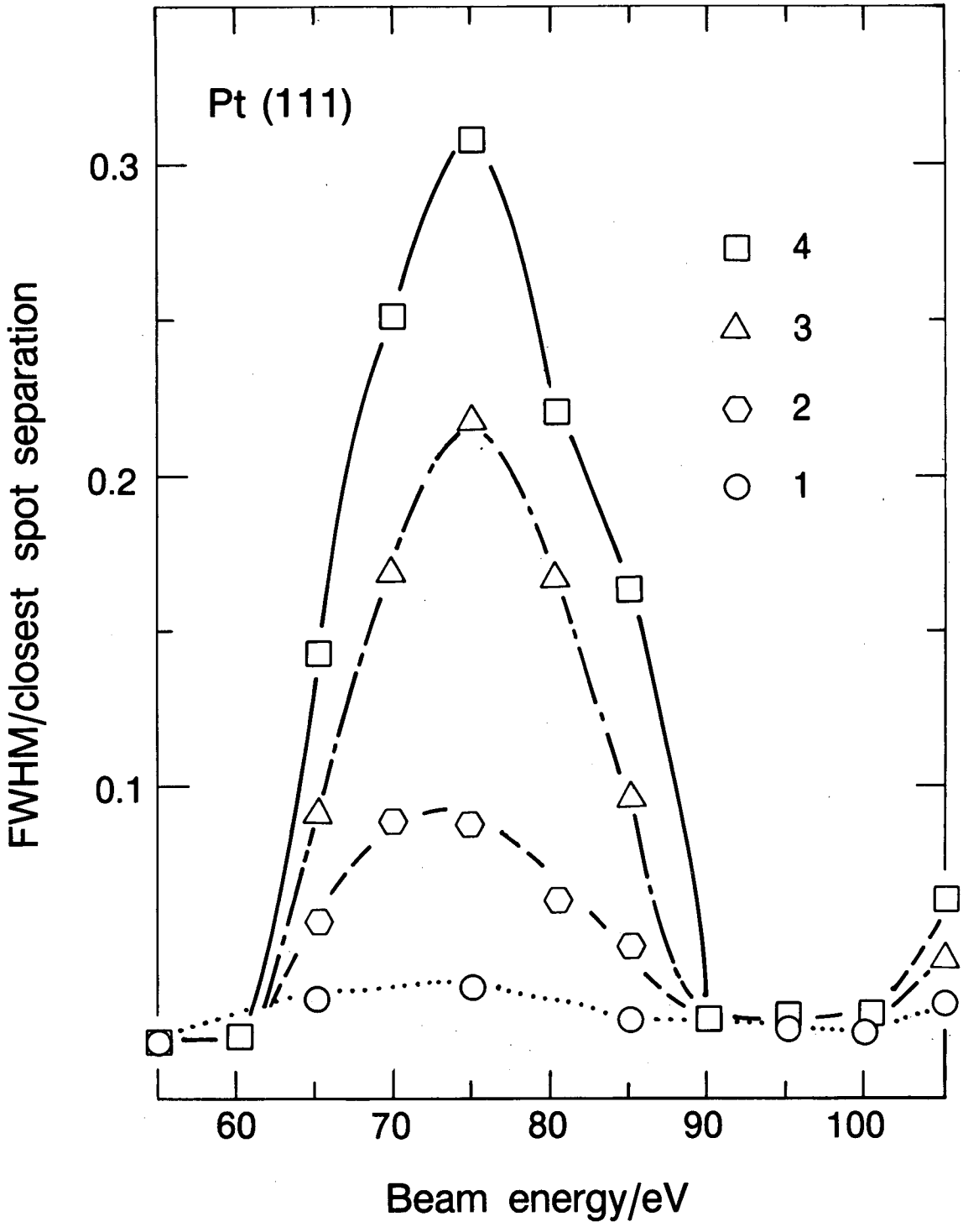

Figure 1b

XBL 8811-9778

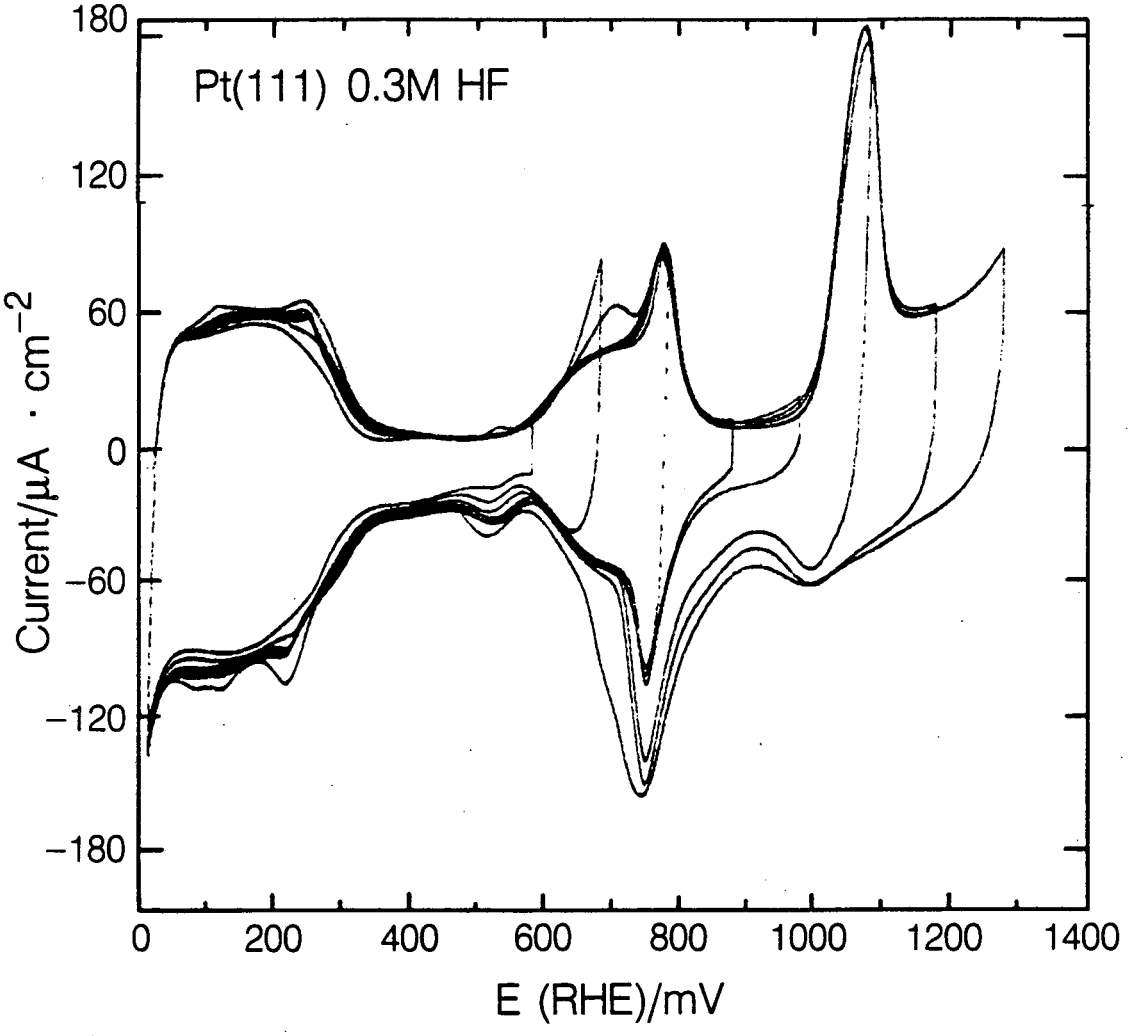

XBL 838-11243

Figure 2

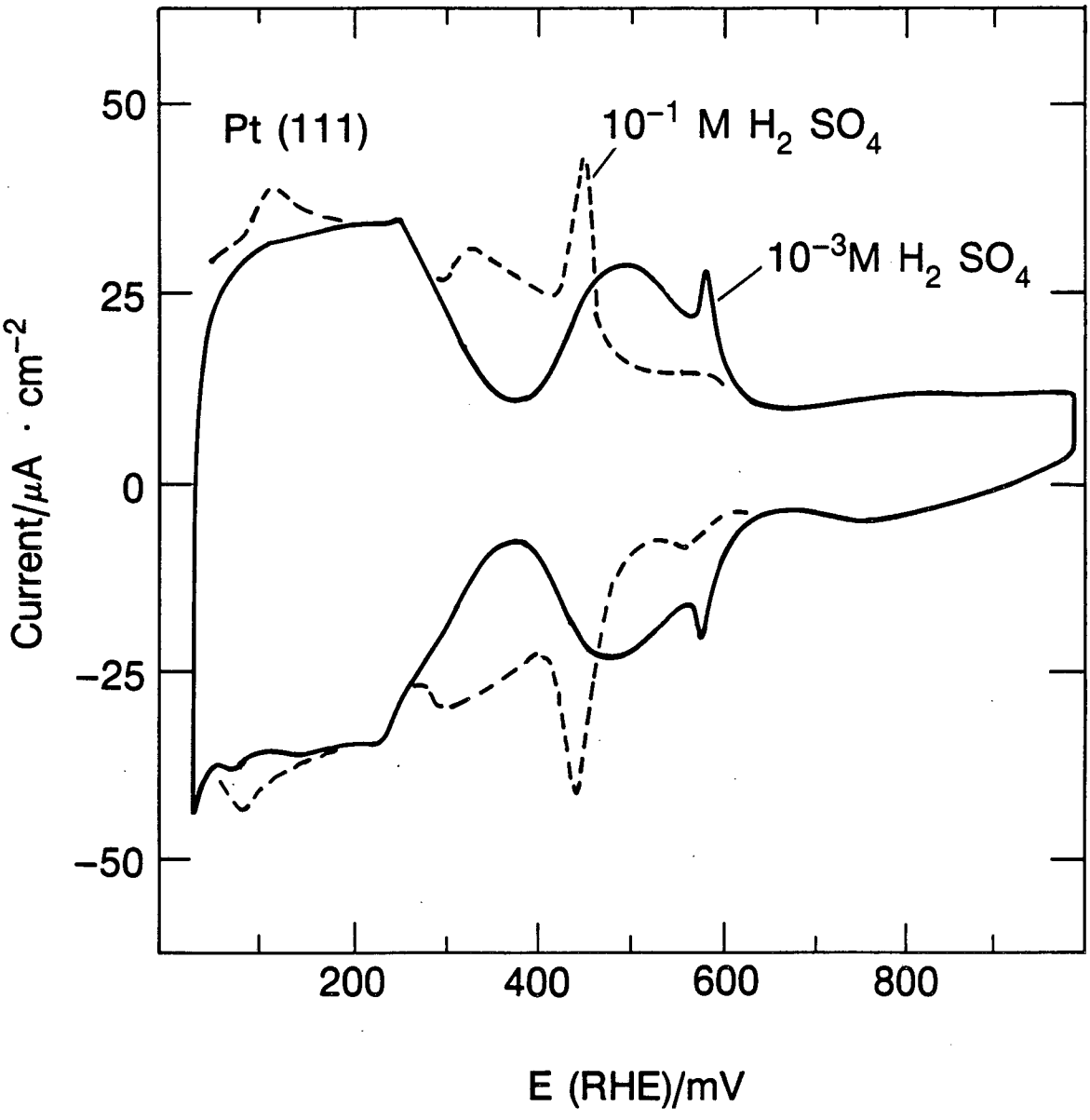

Figure 3

XBL 8811-9780

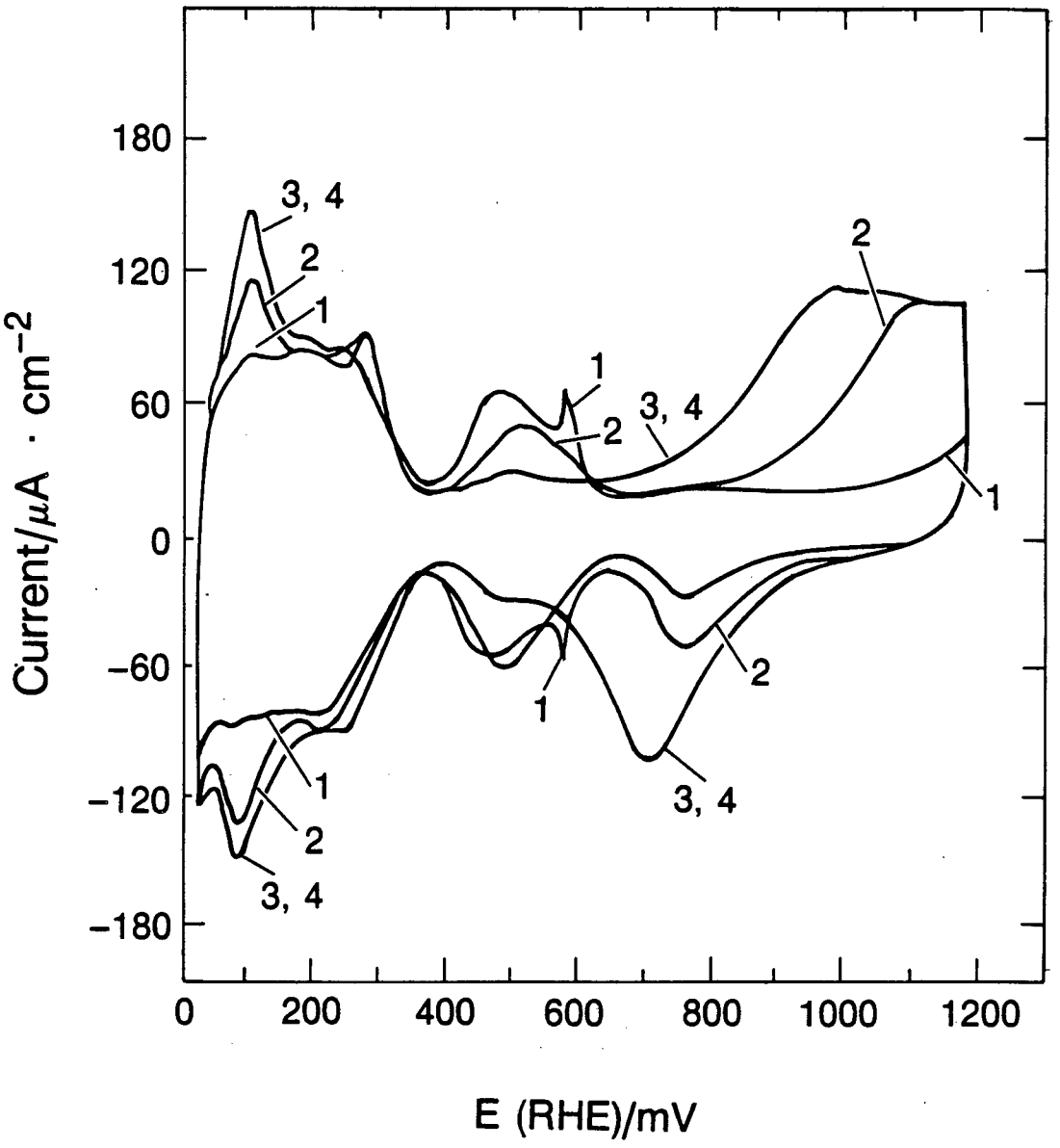

Figure 4

XBL 8811-9777

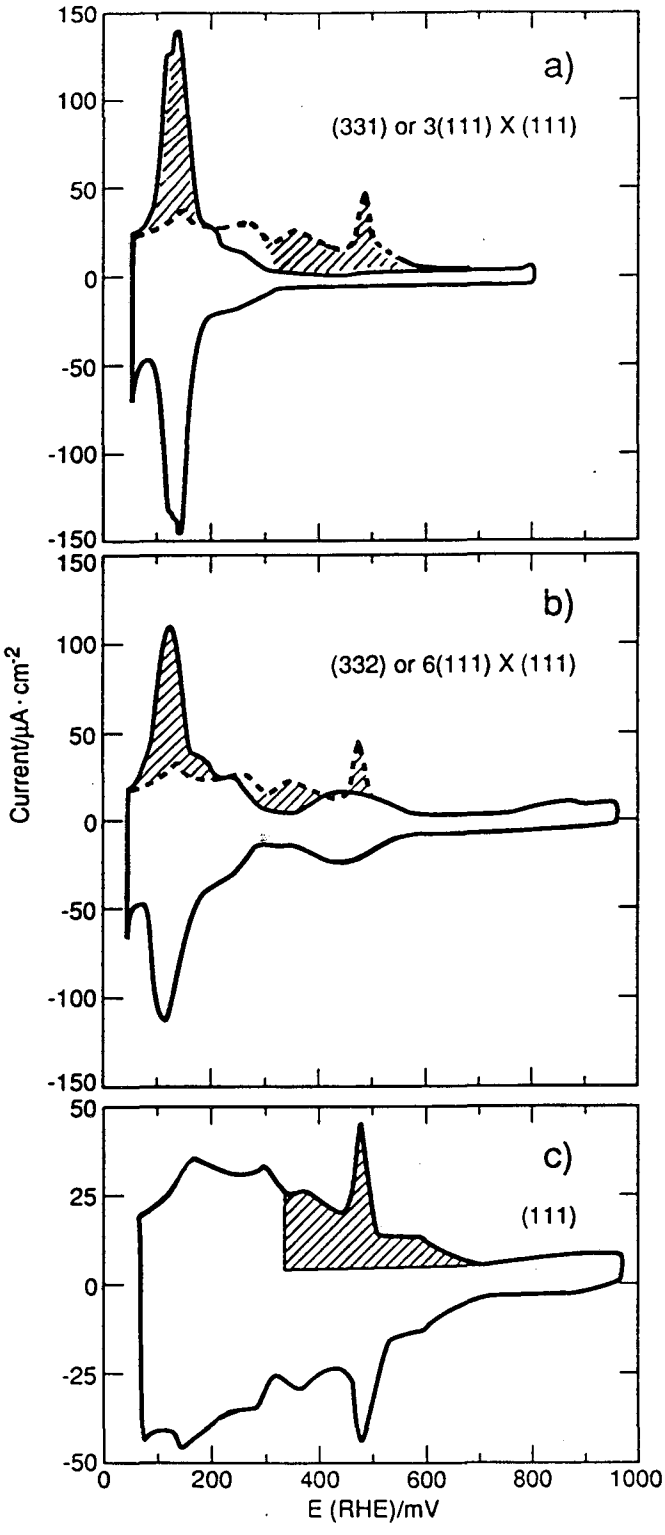
a)
(331) or 3(111) X (111)
b)
(332) or 6(111) X (111)
c)
(111)
Current/μA·cm⁻²
E (RHE)/mV
150
100
50
0
-50
-100
-150
25
-25
0
200
400
600
800
1000
XBL 911-4616

Figure 5

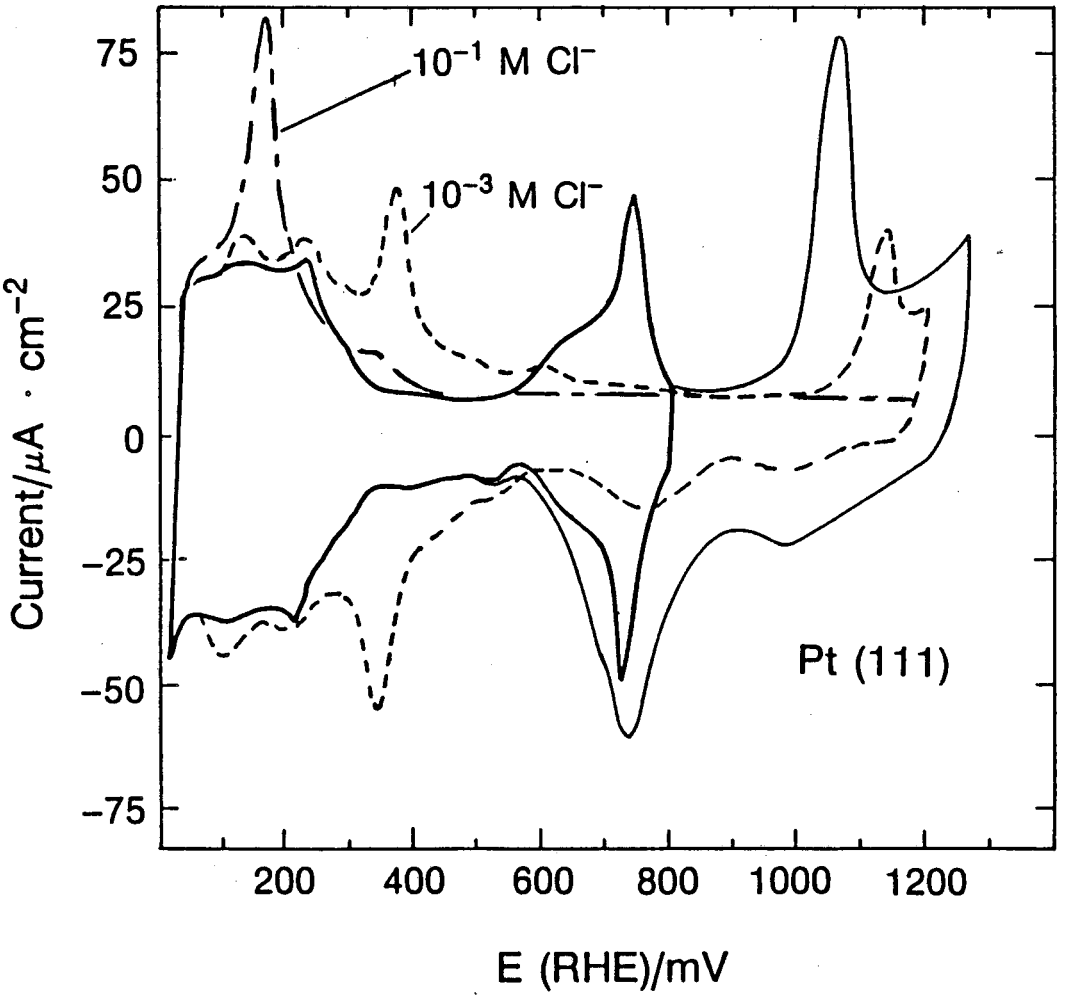

XBL 8811-9776

Figure 6

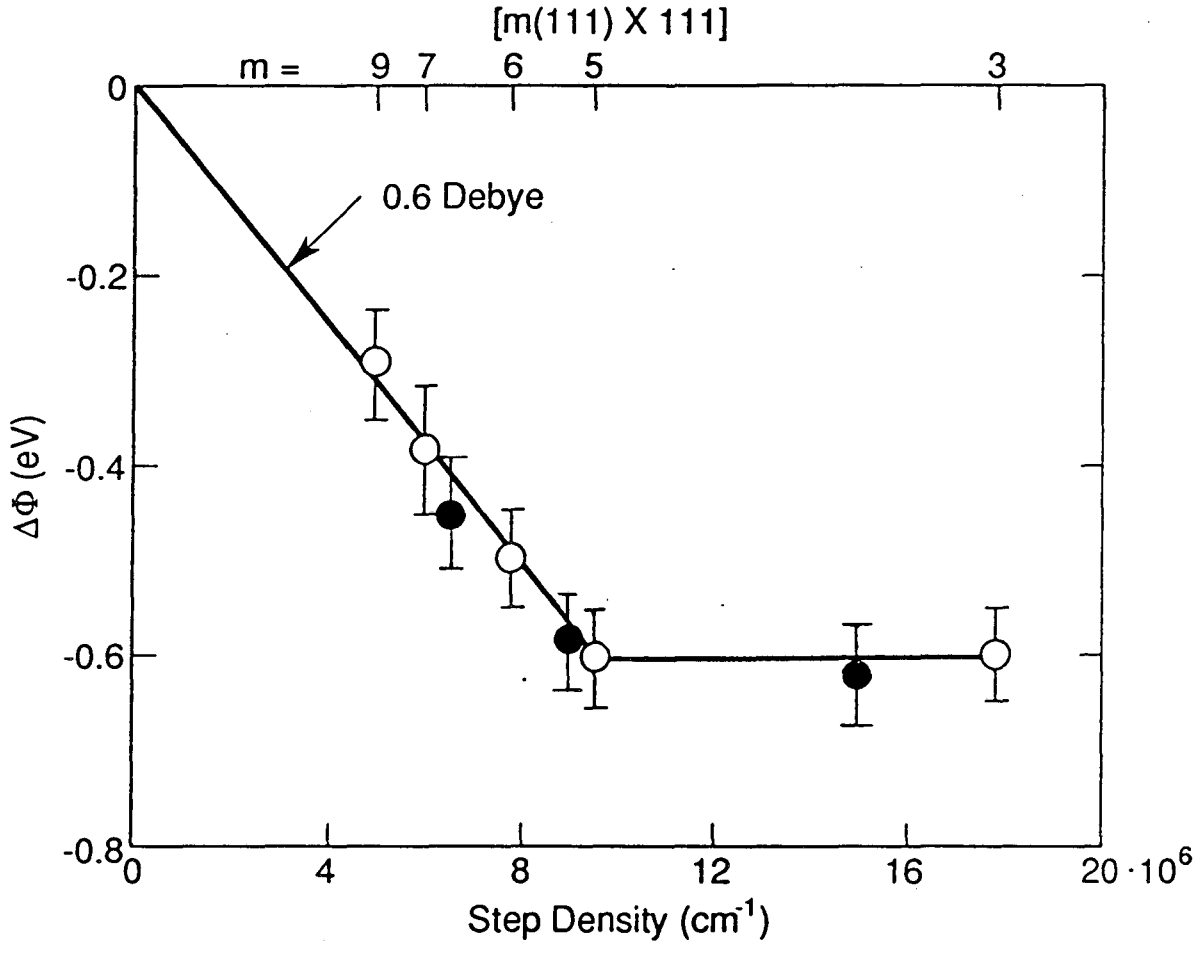

XBL 911-4617

Figure 7

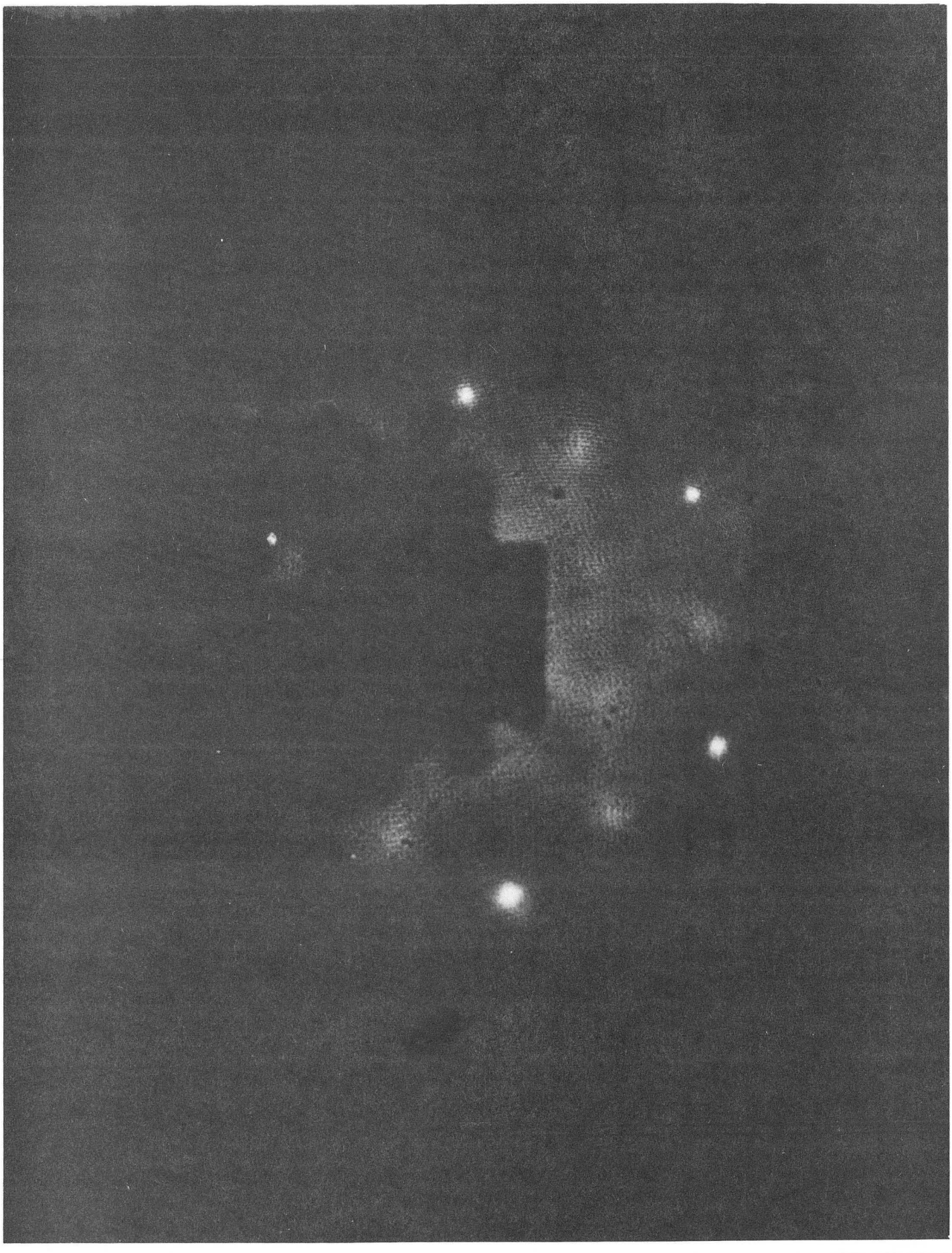

Figure 8a

XBB 880-10296

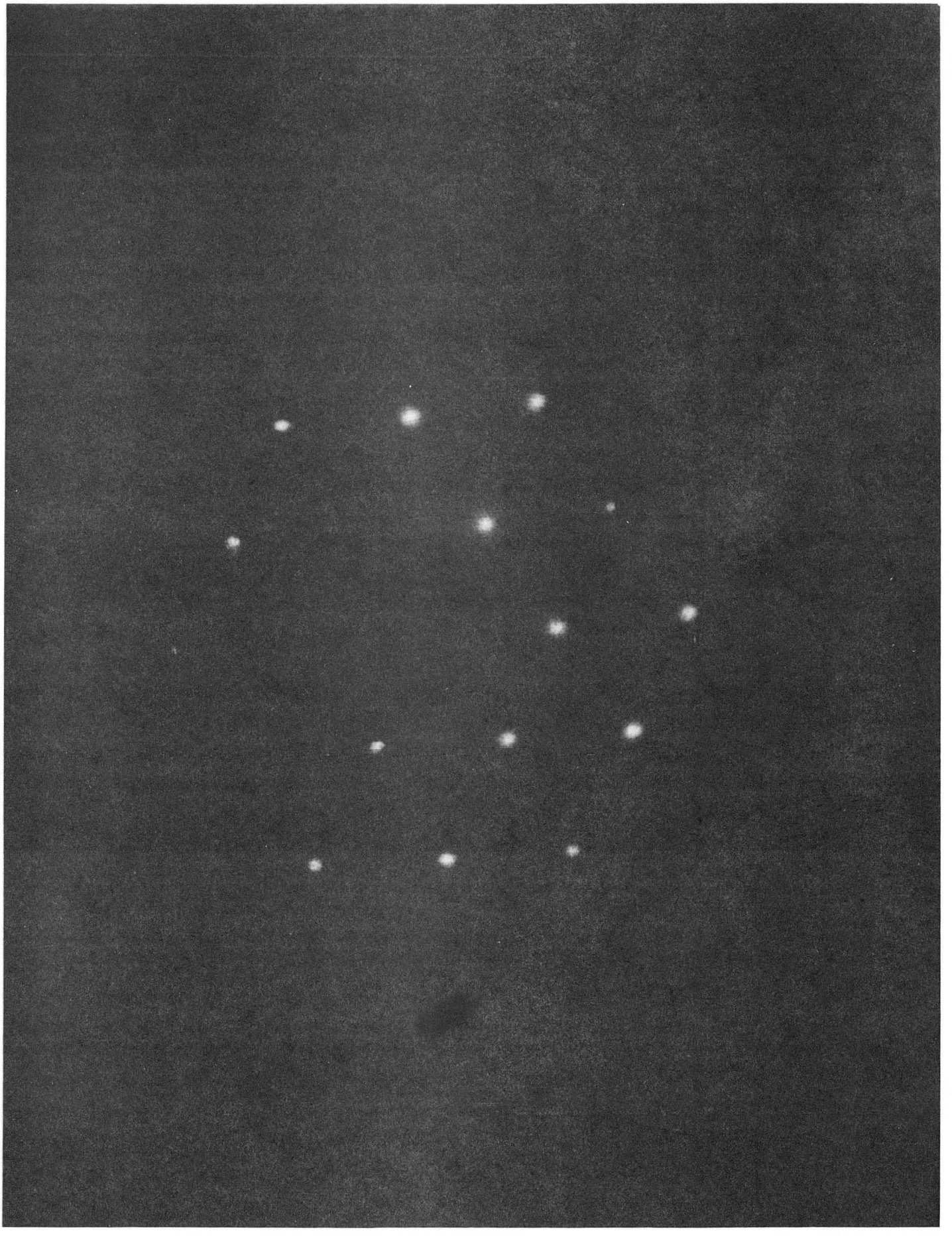

Figure 8b

XBB 880-10291

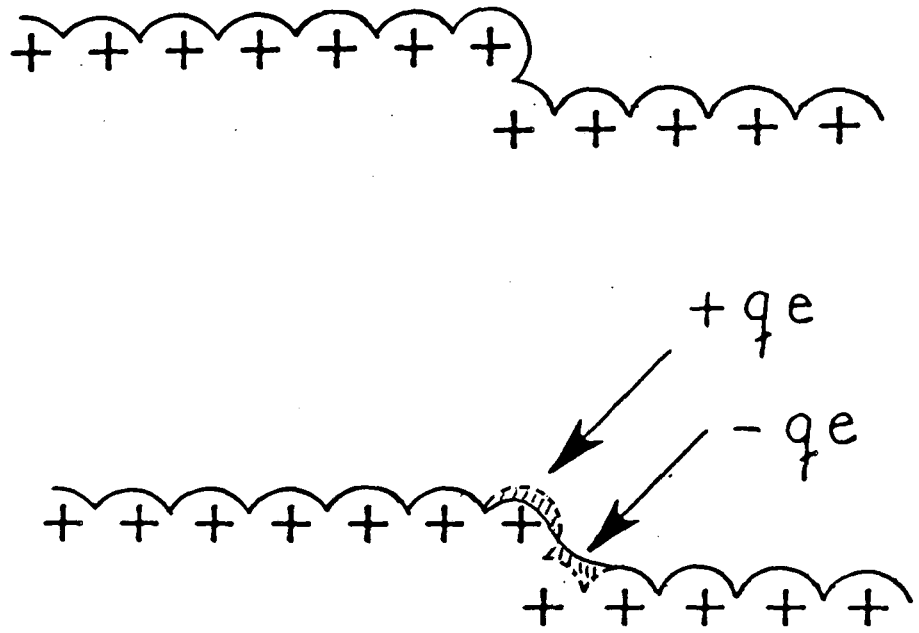

XBL 911-4618

Figure 9

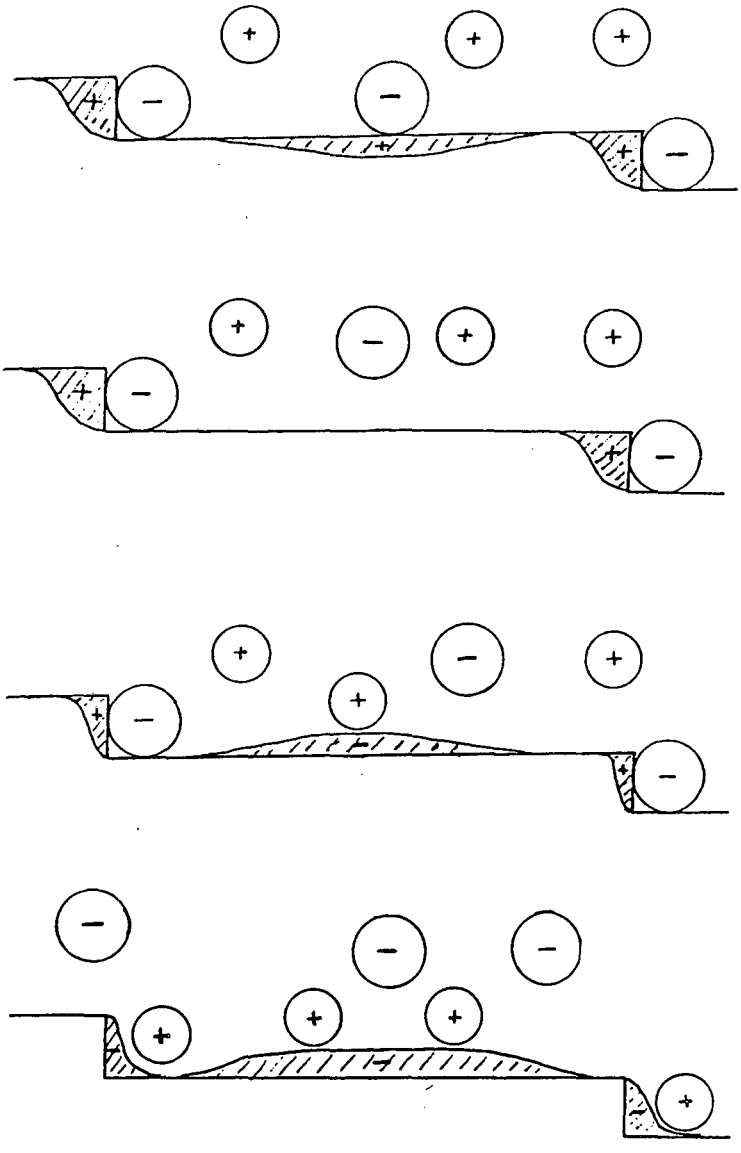

XBL 911-44

Figure 10

LAWRENCE BERKELEY LABORATORY
UNIVERSITY OF CALIFORNIA
INFORMATION RESOURCES DEPARTMENT
BERKELEY, CALIFORNIA 94720